In silico analysis of *IDH3A* gene revealed Novel mutations associated with Retinitis Pigmentosa

Thwayba A. Mahmoud[1*], Abdelrahman H. Abdelmoneim[1], Naseem S. Murshed[1], Zainab O. Mohammed[2], Dina T. Ahmed[1], Fatima A. Altyeb[1], Nuha A. Mahmoud[3], Mayada A. Mohammed[1], Fatima A. Arayah[1], Wafaa I. Mohammed[1], Omnia S. Abayazed[1], Amna S. Akasha[1], Mujahed I. Mustafa[1,4], Mohamed A. Hassan[1]

1- Department of Biotechnology, Africa city of Technology, Sudan

2- Hematology Department, Ribat University Hospital, Sudan

3- Biochemistry Department, faculty of Medicine, National University, Sudan

4- Department of Biochemistry, University of Bahri, Sudan

*Corresponding Author: Thwayba A. Mahmoud, Email: thuwaybaahmed49@gmail.com

Abstract:

Background: *Retinitis Pigmentosa (RP) refers to a group of inherited disorders characterized by the death of photoreceptor cells leading to blindness. The aim of this study is to identify the pathogenic SNPs in the IDH3A gene and their effect on the structure and function of the protein.* ***Method****: we used different bioinformatics tools to predict the effect of each SNP on the structure and function of the protein.* ***Result****: 20 deleterious SNPs out of 178 were found to have a damaging effect on the protein structure and function.* ***Conclusion****: this is the first in silico analysis of IDH3A gene and 20 novel mutations were found using different bioinformatics tools, and they could be used as diagnostic markers for Retinitis Pigmentosa.*

Keywords*:* Retinitis Pigmentosa (RP), *IDH3A*, SNP, *in silico analysis*, diagnostic markers.

1. Introduction

Retinitis Pigmentosa (RP) refers to a group of inherited disorders characterized by the death of photoreceptor cells (rods and cons) leading to blindness (1-12) It affects about 2.5 million people worldwide (5) and symptoms usually starts with night blindness followed by vision loss, progressive restriction of the peripheral visual field and abnormalities in the electroretinogram (1-4, 13). RP is classified as nonsyndromic (70%-80%) (14, 15), syndromic or systemic (4, 16). The most frequent form of syndromic RP is Usher syndrome (14, 17) which involves neurosensory hearing loss, and Bardet-Biedl syndrome (18, 19) which involves RP, obesity, renal abnormalities and mental retardation.

RP has three patterns of inheritance; autosomal dominant (adRP), autosomal recessive (arRP) and X-linked pattern (14, 20-22) and the most reported genes for each case are *RHO* gene, *USH2A* and *RPGR* respectively (4, 21-24) yet the gene we are working on, Isocitrate Dehydrogease 3, (*IDH3A*) is a novel gene identified as the cause of typical arRP (25) located in the human chromosome 15q25.1 (26). The *IDH3A* function is to catalyze the oxidative decarboxylation of isocitrate (27) which is the key rate-limiting step of the tricarboxylic acid cycle. It also plays a central role in the aerobic energy production and cellular respiration thus mutations in this gene will affect the nervous system (28, 29) and may cause cancer (30, 31).

Although the RP is the most common inherited disease of the retina (14, 32-36) there is still no effective therapeutic strategy and the exact pathogenesis and etiology of the disease is not clear (3, 5, 32, 37).

The aim of this study is to identify the pathogenic SNPs in the *IDH3A* gene and their effect on the structure and function of the protein, which might help in the overall understanding of the pathogenesis of the disease and could be used as diagnostic markers. This is the first in silico analysis in the coding region of *IDH3A* gene to prioritize SNPs for further genetic mapping studies. Utilization of in analysis softwares expedites the process of identifying the deleterious SNPs with no cost, and also facilitates future genetic studies.(38)

2. Method

2.1 Data Mining

The data concerning the *IDH3A* human gene was procured from the National Center for Biotechnology Information (NCBI)(http://www.ncbi.nlm.nih.gov/) (39). The SNPs information of the *IDH3A* gene was collected from the NCBI dbSNP database (http://www.ncbi.nlm.nih.gov/snp/) (40) and the IDH3A protein sequence was obtained from UniProt database (https://www.uniprot.org/) (41).

2.2 SIFT

SIFT algorithm predicts damaging and tolerated (non-damaging) substitutions based on sequence homology and physical properties of sequence submitted. It also predicts the functional consequences of amino acid substitutions caused due to nsSNPs. SIFT is based on the premise that protein evolution is correlated with protein function. It uses multiple alignment information to predict tolerated and deleterious substitutions for every position of the sequence of interest. (42, 43)

SIFT score ranges from 0 to 1. The amino acid substitution is predicted to be damaging if the score is ≤ 0.05, and tolerated if the score is > 0.05. (https://sift.bii.a-star.edu.sg/)

2.2 PolyPhen-2

PolyPhen-2 (polymorphism phenotyping v2), available as software and via a Web server, predicts the possible impact of amino acid substitutions on the stability and function of human proteins using structural and comparative evolutionary considerations. PolyPhen-2 uses eight sequence-based and structure-based predictive features which were selected automatically by an interactive greedy algorithm. Majority of these features involves comparison of a property of the wild-type residue and the corresponding property of the mutant.

PolyPhen-2 uses multiple sequence alignment by selecting the homologues sequences for the analysis using a clustering algorithm and then constructs and refines their multiple alignments. The functional significance of an amino acid replacement is predicted from its individual features by Naïve Bayes classifier. (44, 45)

Prediction outcomes are benign, possibly damaging or probably damaging according to the PSIC value which ranges from 0 to 1. Values closer to zero are considered benign while values closer to one are considered probably damaging. PolyPhen-2 is available at (http://genetics.bwh.harvard.edu/pph2/).

2.3 PROVEAN

Provean predicts the functional effect of protein sequence variations, including single amino acid substitutions and small insertions and deletions. The prediction is based on the change, caused by a given variation, in the similarity of a query sequence to a set of its related protein sequences. For this prediction the algorithm is required to compute a semi global pair-wise sequence alignment score between the query sequence and each of the related sequences (46, 47). Provean is available at this website (http://provean.jcvi.org/index.php).

2.4 PhD-SNP

A predictor of human deleterious SNPs based on an online Support Vector Machine (SVM) classifier explicitly designed for human dataset correlated with disease inducing mutations. The SVM classifies mutations into disease related (desired output set to 0) and neutral polymorphism, based on protein sequence and profile information. The reliability index value (RI) is evaluated and the probability of the amino acid being deleterious is obtained. A probability> 0.5 is considered disease associated whereas ≤0.5 is considered neutral. PhD-SNP is available at this website (http://snps.biofold.org/phd-snp/phd-snp.html).

2.5 SNP&GO

SNP&GO is a method for the prediction of deleterious SNPs using protein functional annotation. The server is based on SVM classifier that discriminates between disease related and neutral SNPs. It has two components, one is sequence based and the other is structure based. The output gives the mutated residue, the prediction (either disease or neutral), RI (probability of disease related class) and the information about the prediction method. If the probability is > 0.5 then the variation is disease associated. SNP&GO is available at this website (http://snps.biofold.org/snps-and-go/index.html) (48, 49).

2.6 P-Mut

P-Mut uses a robust methodology to predict disease-associated mutations. It allows fast and accurate prediction based on the use of neural networks (NNs) trained with a large database of neutral mutations and pathological mutations of mutational hot spots which are obtained by alanine scanning, massive mutations and genetically accessible mutations. The final output is displayed as a pathogenecity index ranging from 0 to 1 and a confidence index ranging from 0 to 9(50). P-Mut server is available at this website (http://mmb.irbbarcelona.org/PMut/).

2.7 I-Mutant 3.0

I-Mutant is an SVM-based tool for the automatic prediction of protein stability changes upon single point mutations. The predictions are performed starting either from the protein structure or, more importantly, from the protein sequence. I-Mutant correctly predicts 80% or 77% of the dataset, depending on the usage of structural or sequence information, respectively. The server was also trained to predict the value of the free energy stability change upon single point mutation, starting from the protein structure or sequence (51). (http://gpcr2.biocomp.unibo.it/cgi/predictors/I-Mutant3.0/I-Mutant3.0.cgi)

2.8 MUpro

MUpro is a SVM-based tool for the prediction of protein stability changes upon nsSNPs. The value of the energy change is predicted, and a confidence score between -1 and 1 for measuring the confidence of the prediction is calculated. The accuracy for SVM using sequence information is 84.2%. MUpro is available at (http://mupro.proteomics.ics.uci.edu/).

2.9 Chimera 1.8

Chimera is a highly extensible program of interactive visualization and analysis of molecular structures and related data, including density maps, supramolecular assemblies, sequence alignments, docking results, trajectories and conformational ensembles. High quality images and animations can be generated. Chimera is segmented into a core that provides basic services and visualization, and extensions that provides higher level functionalities (52). The protein structure was obtained from RaptorX server (http://raptorx.uchicago.edu/). Chimera is available at (http://www.cgl.ucsf.edu/chimera/).

2.10 GeneMania

GeneMania is a flexible, user-friendly web interface for generating hypothesis about gene function, analyzing gene lists and prioritizing genes for functional assays. Given a query gene list, GeneMania finds functionally similar genes using a wealth of genomics and proteomics data. Another use of GeneMania is gene function prediction by finding the genes that are likely to share functions with the query based on their interactions with it (53-55). (https://genemania.org/).

2.11 Project HOPE

Project HOPE is next-generation web application for automatic mutant analysis and it explains the molecular origin of a disease related phenotype caused by mutations in human proteins. HOPE collects information from data

sources such as the protein's 3D structure and the UniProt database of well-annotated protein sequences. A decision scheme is used to process these data and to predict the effect of the mutation on the 3D structure and the function of the protein. Then a report is produced which explains and illustrate the effect of the mutations (56). (http://www.cmbi.ru.nl/hope/method/)

2.12 BioEdit

BioEdit is a user-friendly sequence alignment editor which enables the user to manually edit a multiple sequence alignment in order to obtain a more reasonable or expected alignment. The sequences are entered in a FastA format and the output file is provided in a suitable user-designated format. BioEdit is available for download at (http://www.mbio.ncsu.edu/bioedit/bioedit.html).

3. Result:

Table (1): Deleterious (damaging) nsSNPs predicted by various softwares:

Amino acid change	SIFT		Polyphen-2		PROVEAN	
	prediction	score	prediction	score	prediction	score
G39V	affect	0	probably damaging	1	Deleterious	-8.482
I46S	affect	0	probably damaging	1	Deleterious	-5.655
V50F	affect	0	probably damaging	1	Deleterious	-4.679
G97C	affect	0	probably damaging	1	Deleterious	-8.624
A122T	affect	0	probably damaging	1	Deleterious	-3.904
A122S	affect	0	probably damaging	1	Deleterious	-2.908
A122E	affect	0	probably damaging	1	Deleterious	-4.887
T172I	affect	0	probably damaging	1	Deleterious	-5.824
R178C	affect	0	probably damaging	1	Deleterious	-7.443
R178H	affect	0	probably damaging	1	Deleterious	-4.459
F184L	affect	0	probably damaging	1	Deleterious	-5.924
Y186C	affect	0	probably damaging	1	Deleterious	-8.131
V198G	affect	0	probably damaging	1	Deleterious	-6.794
L210P	affect	0	probably damaging	1	Deleterious	-6.487
P243R	affect	0	probably damaging	1	Deleterious	-8.773

G268R	affect	0	probably damaging	1	Deleterious	-7.8
G271S	affect	0	probably damaging	1	Deleterious	-5.827
A302V	affect	0	Probably Damaging	1	Deleterious	-3.887
P304H	affect	0	probably damaging	1	Deleterious	-8.715
I327T	Affect	0	probably damaging	1	Deleterious	-4.766

Table (2): Disease-associated nsSNPs predicted by various softwares:

sub	PhD-SNP prediction	RI	score	SNP&GO prediction	RI	score	P-Mut prediction	score
G39V	Disease	8	0.914	Disease	7	0.826	Disease	0.93 (94%)
I46S	Disease	7	0.864	Disease	1	0.552	Disease	0.93 (94%)
V50F	Disease	7	0.829	Disease	7	0.854	Disease	0.93 (94%)
G97C	Disease	8	0.898	Disease	7	0.835	Disease	0.93 (94%)
A122T	Disease	4	0.706	Disease	4	0.679	Disease	0.70 (86%)
A122S	Disease	5	0.757	Disease	4	0.686	Disease	0.75 (87%)
A122E	Disease	7	0.868	Disease	6	0.813	Disease	0.93 (94%)
T172I	Disease	7	0.841	Disease	5	0.74	Disease	0.93 (94%)
R178C	Disease	8	0.914	Disease	6	0.788	Disease	0.93 (94%)
R178H	Disease	7	0.857	Disease	4	0.704	Disease	0.88 (92%)
Y186C	Disease	7	0.836	Disease	4	0.71	Disease	0.93 (94%)
V198G	Disease	7	0.827	Disease	4	0.717	Disease	0.87 (91%)
L210P	Disease	9	0.933	Disease	8	0.878	Disease	0.93 (94%)
P243R	Disease	8	0.882	Disease	5	0.751	Disease	0.93 (94%)
G268R	Disease	8	0.913	Disease	7	0.854	Disease	0.93 (94%)
G271S	Disease	8	0.922	Disease	7	0.86	Disease	0.92 (94%)
P304H	Disease	8	0.876	Disease	5	0.74	Disease	0.93 (94%)

I327T	Disease	6	0.792	Disease	5	0.769	Disease	0.93 (94%)

Table (3): The effect of the deleterious SNPs on the stability predicted by 2 softwares:

Amino acid change	SVM2 Prediction Effect	RI	DDG Value Prediction	Mupro prediction	Mupro score
G39V	Decrease	5	-0.26	Decrease	-0.95687971
I46S	Decrease	9	-1.97	Decrease	-1.2674836
V50F	Decrease	7	-0.99	Decrease	-1.4400617
G97C	Decrease	7	-0.90	Decrease	-0.37395268
A122T	Decrease	7	-0.87	Decrease	-0.91965426
A122S	Decrease	9	-0.94	Decrease	-0.75236358
A122E	Decrease	3	-0.62	Decrease	-0.46426725
T172I	Decrease	4	-0.33	Decrease	-0.15840056
R178C	Decrease	0	-0.61	Decrease	-0.63648418
R178H	Decrease	6	-1.02	Decrease	-1.1281043
Y186C	Decrease	0	-1.13	Decrease	-0.72393174
V198G	Decrease	9	-2.09	Decrease	-2.7354434
L210P	Decrease	8	-2.08	Decrease	-2.4575871
P243R	Decrease	4	-0.87	Decrease	-0.37063631
G268R	Decrease	3	-0.48	Decrease	-0.76962057
G271S	Decrease	3	-0.97	Decrease	-0.22864936
P304H	Decrease	7	-1.35	Decrease	-0.72552786
I327T	Decrease	8	-1.67	Decrease	-1.3879025

Table (4): *IDH3A*gene function and its appearance in network and genome:

Function	FDR	Genes in network	Genes in genome
tricarboxylic acid cycle	1.20E-12	7	21
aerobic respiration	2.19E-11	7	33
energy derivation by oxidation of organic compounds	4.26E-08	9	285
cellular respiration	4.30E-07	7	140

mitochondrial matrix	5.43E-07	8	257
tricarboxylic acid metabolic process	1.05E-06	4	11
oxidoreductase activity, acting on the CH-OH group of donors, NAD or NADP as acceptor	0.002837	4	73
proteasome accessory complex	0.002932	3	20
oxidoreductase activity, acting on CH-OH group of donors	0.003524	4	82
regulation of cellular ketone metabolic process	0.019321	4	129
proteasome complex	0.038133	3	51
regulation of cellular amino acid metabolic process	0.04157	3	57
DNA damage response, signal transduction by p53 class mediator resulting in cell cycle arrest	0.04157	3	67
signal transduction involved in mitotic DNA damage checkpoint	0.04157	3	68
cell cycle arrest	0.04157	4	191
signal transduction involved in DNA integrity checkpoint	0.04157	3	68
negative regulation of ubiquitin-protein ligase activity involved in mitotic cell cycle	0.04157	3	67
signal transduction involved in mitotic G1 DNA damage checkpoint	0.04157	3	67
signal transduction involved in mitotic DNA integrity checkpoint	0.04157	3	68
regulation of cellular amine metabolic process	0.04157	3	67
cellular ketone metabolic process	0.04157	4	166
signal transduction involved in mitotic cell cycle checkpoint	0.04157	3	68
signal transduction involved in DNA damage checkpoint	0.04157	3	68
intracellular signal transduction involved in G1 DNA damage checkpoint	0.04157	3	67
signal transduction involved in cell cycle checkpoint	0.041693	3	69
positive regulation of ubiquitin-protein ligase activity involved in mitotic cell cycle	0.041806	3	72
antigen processing and presentation of exogenous peptide antigen via MHC class I, TAP-dependent	0.041806	3	75
mitotic G1 DNA damage checkpoint	0.041806	3	74
negative regulation of ubiquitin-protein ligase activity	0.041806	3	71
G1 DNA damage checkpoint	0.041806	3	75
negative regulation of ligase activity	0.041806	3	71
mitotic G1/S transition checkpoint	0.041806	3	74
antigen processing and presentation of exogenous peptide antigen via MHC class I	0.044238	3	78
regulation of ubiquitin-protein ligase activity involved in mitotic cell cycle	0.044238	3	78
2-oxoglutarate metabolic process	0.04747	2	13
positive regulation of cell cycle arrest	0.048104	3	83
anaphase-promoting complex-dependent proteasomal ubiquitin-dependent protein catabolic process	0.048104	3	83
positive regulation of ubiquitin-protein ligase activity	0.048104	3	84
mitotic DNA damage checkpoint	0.048104	3	84

mitotic DNA integrity checkpoint	0.050796	3	87
positive regulation of ligase activity	0.050796	3	87
negative regulation of G1/S transition of mitotic cell cycle	0.056677	3	91
antigen processing and presentation of peptide antigen via MHC class I	0.060955	3	94
negative regulation of protein ubiquitination	0.063409	3	96
regulation of ubiquitin-protein ligase activity	0.063935	3	97
regulation of cell cycle arrest	0.066996	3	100
regulation of ligase activity	0.066996	3	100
DNA damage response, signal transduction by p53 class mediator	0.084641	3	109
regulation of G1/S transition of mitotic cell cycle	0.087485	3	111
negative regulation of cell cycle	0.090561	4	290

Table (5): The gene co-expressed, shared domain and interaction with IDH3A gene network:

Gene 1	Gene 2	Weight	Network group
PRKAB2	NCS1	0.025968712	Co-expression
PSMD4	ACO2	0.008735185	Co-expression
SUCLA2	IDH3A	0.01131356	Co-expression
PSMD13	IDH3B	0.012056911	Co-expression
PSMC2	SDHB	0.015322111	Co-expression
PSMD4	PSMD13	0.011086262	Co-expression
ACO2	IDH3A	0.01753294	Co-expression
IDH2	ACO2	0.018662373	Co-expression
SDHB	IDH3A	0.014610451	Co-expression
PSMC2	IDH1	0.006490774	Co-expression
PSMC2	SUCLA2	0.008042993	Co-expression
PSMC2	PSMD13	0.004759985	Co-expression
HSD17B10	SDHB	0.012080309	Co-expression
UBR2	SUCLA2	0.00804327	Co-expression
HSD17B10	PSMD13	0.019187195	Co-expression
IDH2	IDH3A	0.01316396	Co-expression
PSMD13	IDH3A	0.013595836	Co-expression
PSMD13	RRM1	0.010043109	Co-expression
IDH3B	IDH3G	0.003032382	Co-expression
ACO2	IDH3G	0.002506605	Co-expression
ACO2	IDH3B	0.002463074	Co-expression

SDHB	IDH3A	0.00955701	Co-expression
PSMD13	ACO2	0.0061027	Co-expression
PSMC2	SDHB	0.012523267	Co-expression
PSMD4	IDH3G	0.007240255	Co-expression
PSMD4	PSMD13	0.023427771	Co-expression
DMWD	LONP1	0.01685009	Co-expression
PSMD13	IDH3G	0.005043003	Co-expression
GFPT2	NCS1	0.014308699	Co-expression
PSMC2	PSMD13	0.004028172	Co-expression
ACO2	IDH3G	0.009149939	Co-expression
RRM1	IDH3A	0.004243086	Co-expression
SDHB	IDH3B	0.012938852	Co-expression
PSMD13	IDH3A	0.004226407	Co-expression
PSMC2	SDHB	0.012219397	Co-expression
PSMD4	IDH3B	0.012593607	Co-expression
SDHB	IDH3G	0.00731654	Co-expression
S100A16	PSMD13	0.012244721	Co-expression
PSMD4	IDH2	0.007600673	Co-expression
HSD17B10	IDH3B	0.005865612	Co-expression
SUCLA2	IDH3A	0.00993828	Co-expression
PSMC2	SUCLA2	0.00910157	Co-expression
PSMD4	PSMD13	0.022165682	Co-expression
UBR2	RRM1	0.009189893	Co-expression
UBR2	SUCLA2	0.013479872	Co-expression
SDHB	IDH3G	0.006562491	Co-expression
PSMD4	IDH3B	0.019293038	Co-expression
HSD17B10	PSMD13	0.013754741	Co-expression
HSD17B10	IDH2	0.011895314	Co-expression
HSD17B10	SDHB	0.005913078	Co-expression
UBR2	SUCLA2	0.005792231	Co-expression
PSMC2	UBR2	0.003905292	Co-expression
ACO2	IDH3G	0.009078884	Co-localization
SUCLA2	ACO2	0.009040781	Co-localization
PSMD4	PSMC2	0.013745859	Co-localization
IDH3G	IDH3A	0.5	Pathway
IDH3B	IDH3A	0.5	Pathway
IDH3B	IDH3G	0.5	Pathway
PSMC2	PSMD13	0.010244244	Pathway
PSMD4	PSMD13	0.009817638	Pathway
PSMD4	PSMC2	0.009817638	Pathway
IDH3G	IDH3A	0.36939806	Pathway
IDH3B	IDH3A	0.36939806	Pathway
IDH3B	IDH3G	0.36939806	Pathway

ADRA2B	IDH3A	0.17851914	Pathway
ADRA2B	IDH3G	0.17851914	Pathway
ADRA2B	IDH3B	0.17851914	Pathway
ADRA2B	ACO2	0.45970085	Pathway
IDH2	ADRA2B	0.45970085	Pathway
IDH1	ADRA2B	0.45970085	Pathway
PSMC2	PSMD13	0.019868134	Pathway
PSMD4	PSMD13	0.018246995	Pathway
PSMD4	PSMC2	0.018246995	Pathway
HSD17B10	IDH3A	0.09534626	Physical Interactions
HSD17B10	SDHB	0.09534626	Physical Interactions
HSD17B10	IDH1	0.09534626	Physical Interactions
PSMC2	PSMD13	0.029418202	Physical Interactions
PSMD4	PSMD13	0.044049248	Physical Interactions
PSMD4	PSMC2	0.068895765	Physical Interactions
SUCLA2	IDH3A	0.28981236	Physical Interactions
SUCLA2	RRM1	0.10039486	Physical Interactions
S100A16	IDH3A	0.18698043	Physical Interactions
S100A16	SUCLA2	0.035511	Physical Interactions
PSMC2	PSMD13	0.017931806	Physical Interactions
PSMD4	PSMD13	0.026062917	Physical Interactions
PSMD4	PSMC2	0.019284137	Physical Interactions
IDH3G	IDH3A	0.07986558	Physical Interactions
ACO2	IDH3A	0.03645369	Physical Interactions
ACO2	IDH3G	0.11627895	Physical Interactions
IDH2	IDH3A	0.082487226	Physical Interactions
IDH2	IDH3G	0.26311544	Physical Interactions
IDH2	IDH3B	0.37382644	Physical Interactions
IDH1	IDH3A	0.03698435	Physical Interactions
IDH1	IDH3G	0.11797164	Physical Interactions
IDH1	IDH3B	0.16761054	Physical Interactions
IDH1	IDH2	0.121844135	Physical Interactions
SUCLA2	IDH3A	0.053096037	Physical Interactions
SUCLA2	SDHB	0.037427563	Physical Interactions
PSMC2	SUCLA2	0.03408626	Physical Interactions
PSMC2	PSMD13	0.015931962	Physical Interactions
PSMC2	UBR2	0.12044566	Physical Interactions
PSMD4	PSMD13	0.015330697	Physical Interactions
PSMD4	PSMC2	0.009929497	Physical Interactions
PSMD4	IDH3A	0.21221644	Physical Interactions
PSMD4	ACO2	0.11614202	Physical Interactions
PSMD4	PSMC2	0.008754239	Physical Interactions
DMWD	IDH3A	0.19821295	Physical Interactions

IDH3G	IDH3A	0.48433933	Physical Interactions
IDH3B	IDH3A	0.27827385	Physical Interactions
IDH3B	IDH3G	0.37709498	Physical Interactions
PSMC2	PSMD13	0.041475	Physical Interactions
PSMD4	PSMD13	0.01929217	Physical Interactions
PSMD4	PSMC2	0.027964184	Physical Interactions
PSMC2	PSMD13	0.071311645	Physical Interactions
IDH3G	IDH3A	0.5598326	Physical Interactions
IDH3B	IDH3A	0.31132385	Physical Interactions
IDH3B	IDH3G	0.3837958	Physical Interactions
IDH3G	IDH3A	0.6050275	Predicted
ACO2	IDH3A	0.6050275	Predicted
PSMD13	IDH3A	0.09448411	Predicted
GFPT2	IDH3A	0.088868976	Predicted
PSMC2	IDH3A	0.07598789	Predicted
PSMC2	PSMD13	0.043856904	Predicted
PSMC2	GFPT2	0.041250512	Predicted
PSMD4	PSMD13	0.053685274	Predicted
PSMD4	GFPT2	0.05049479	Predicted
PSMD4	PSMC2	0.04317584	Predicted
IDH3G	IDH3A	0.08541127	Predicted
PSMD13	RRM1	0.0637244	Predicted
PRKAB2	IDH3A	0.09472077	Predicted
PSMC2	PSMD13	0.018272607	Predicted
PSMC2	UBR2	0.03779125	Predicted
PSMD4	PSMD13	0.013606428	Predicted
PSMD4	GFPT2	0.014111334	Predicted
PSMD4	PSMC2	0.009794544	Predicted
LONP1	IDH3A	0.09780165	Predicted
ACO2	IDH3G	0.005434668	Predicted
SDHB	IDH3G	0.013495129	Predicted
NCS1	IDH3A	0.2678433	Predicted
SUCLA2	SDHB	0.19398284	Predicted
GFPT2	ACO2	0.005000946	Predicted
GFPT2	PSMD13	0.009550334	Predicted
PRKAB2	IDH3A	0.055580806	Predicted
UBR2	GFPT2	0.011691964	Predicted
PSMC2	IDH2	0.024308747	Predicted
PSMD4	IDH3A	0.009834603	Predicted
PSMD4	ACO2	0.008134047	Predicted
LONP1	IDH3A	0.020420713	Predicted
LONP1	ACO2	0.016889654	Predicted
LONP1	GFPT2	0.015867962	Predicted

LONP1	PSMD4	0.025809262	Predicted
RRM1	IDH3A	0.61784995	Predicted
SDHB	IDH3A	0.44045475	Predicted
IDH1	IDH2	0.68125004	Predicted
IDH3G	IDH3A	0.76401514	Predicted
PSMD4	PSMD13	0.2537096	Predicted
PSMD4	PSMC2	0.2537096	Predicted
IDH3B	IDH3A	0.0635202	Predicted
ACO2	IDH3A	0.04223968	Predicted
SUCLA2	IDH3B	0.08028842	Predicted
IDH3G	IDH3A	1	Predicted
IDH3G	IDH3A	0.851885	Predicted
PSMC2	PSMD13	0.049788807	Predicted
PSMD4	PSMD13	0.041182987	Predicted
PSMD4	PSMC2	0.057894204	Predicted
IDH3B	IDH3A	1	Predicted
IDH3G	IDH3A	0.7349278	Predicted
NCS1	IDH3A	0.3738891	Predicted
UBR2	IDH3A	0.7409567	Predicted
IDH3G	IDH3A	0.46697527	Predicted
IDH3B	IDH3A	0.46697527	Predicted
IDH3B	IDH3G	0.5505102	Predicted
IDH3B	IDH3A	0.7450433	Predicted
IDH3G	IDH3A	0.29863566	Shared protein domains
IDH3B	IDH3A	0.29863566	Shared protein domains
IDH3B	IDH3G	0.29863566	Shared protein domains
IDH2	IDH3A	0.2069319	Shared protein domains
IDH2	IDH3G	0.2069319	Shared protein domains
IDH2	IDH3B	0.2069319	Shared protein domains
IDH1	IDH3A	0.2069319	Shared protein domains
IDH1	IDH3G	0.2069319	Shared protein domains
IDH1	IDH3B	0.2069319	Shared protein domains
IDH1	IDH2	0.36203977	Shared protein domains
S100A16	NCS1	0.005545437	Shared protein domains
LONP1	PSMC2	0.010929901	Shared protein domains
IDH3G	IDH3A	0.25	Shared protein domains
IDH3B	IDH3A	0.25	Shared protein domains
IDH3B	IDH3G	0.25	Shared protein domains
IDH2	IDH3A	0.25	Shared protein domains
IDH2	IDH3G	0.25	Shared protein domains
IDH2	IDH3B	0.25	Shared protein domains
IDH1	IDH3A	0.25	Shared protein domains
IDH1	IDH3G	0.25	Shared protein domains

IDH1	IDH3B	0.25	Shared protein domains
IDH1	IDH2	0.25	Shared protein domains
S100A16	NCS1	0.006626467	Shared protein domains
LONP1	PSMC2	0.018407136	Shared protein domains

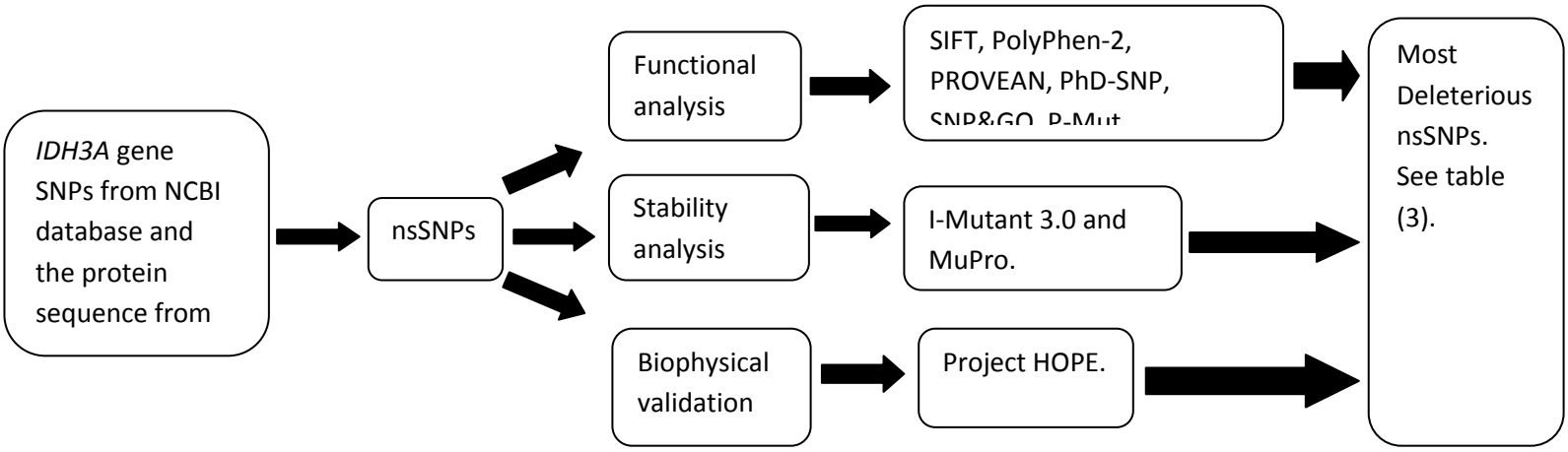

Figure 1: Diagrammatic representation of the *IDH3A* gene in silico work flow.

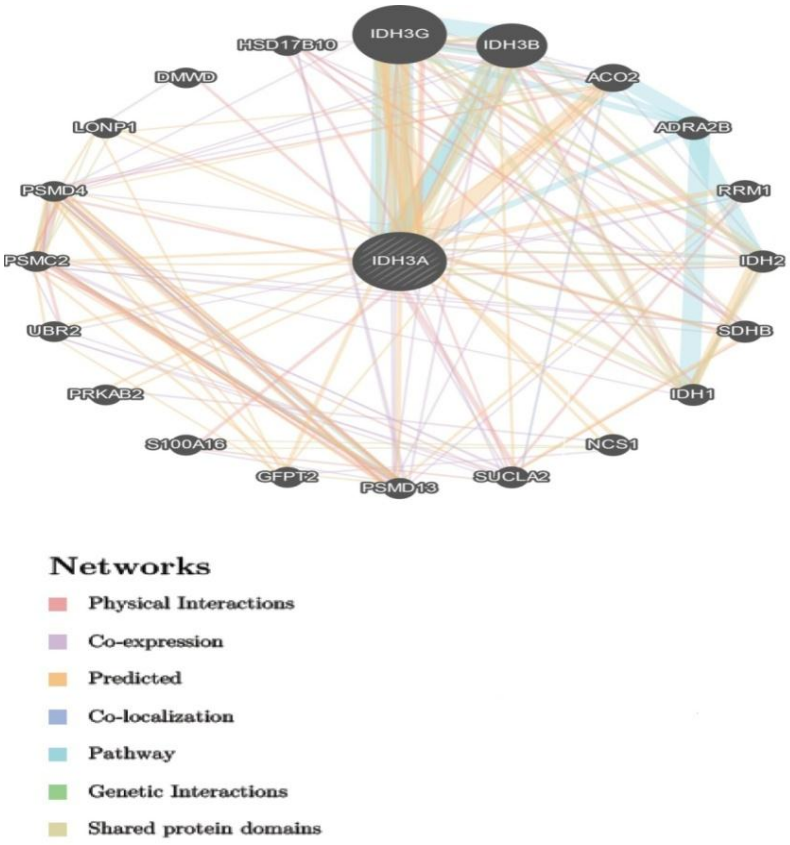

Figure 2: Interaction of *IDH3A* gene with its related genes.

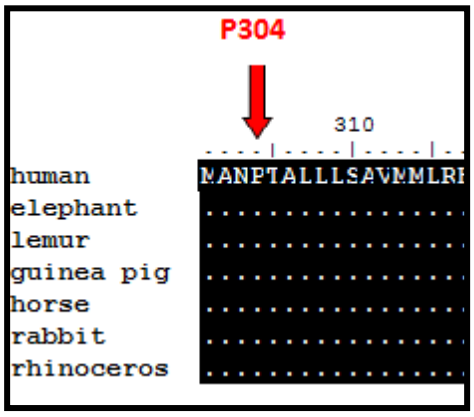

Figure 3: Alignment of 7 amino acid sequences of *IDH3A* gene shows that the residue predicted to be mutated in our study (pointed at by a red arrow) is actually found in a conserved region across species. Sequence alignment was done using BioEdit software (v7.2.5).

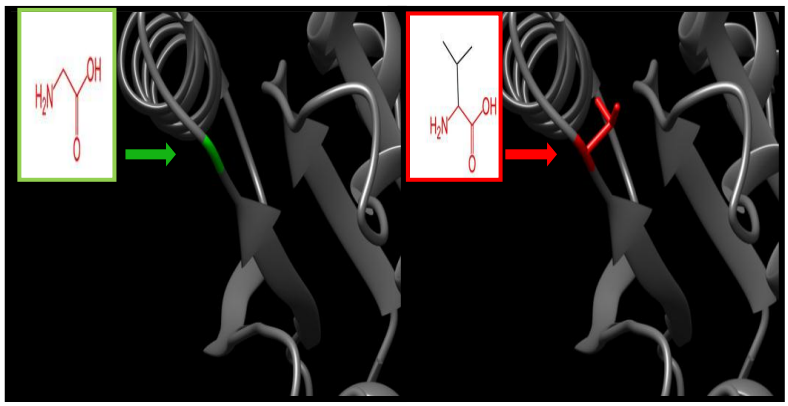

Figure 4: (rs1465252689) (G39V) the amino acid Glycine changes to Valine at position 39.

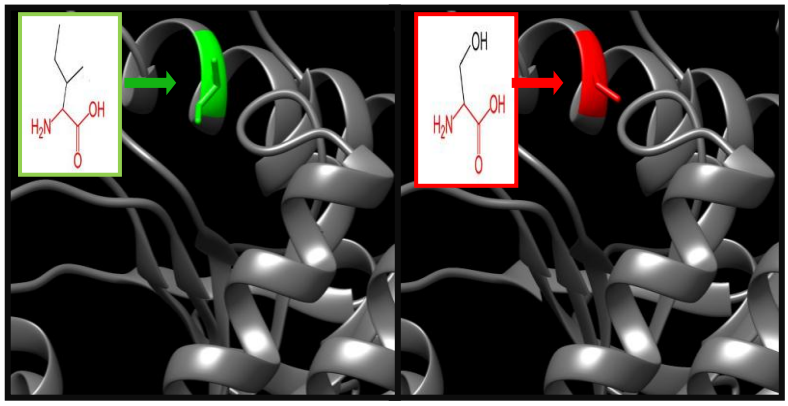

Figure 5: (rs1271001430) (I46S) the amino acid Isoleucine changes to Serine at position 46.

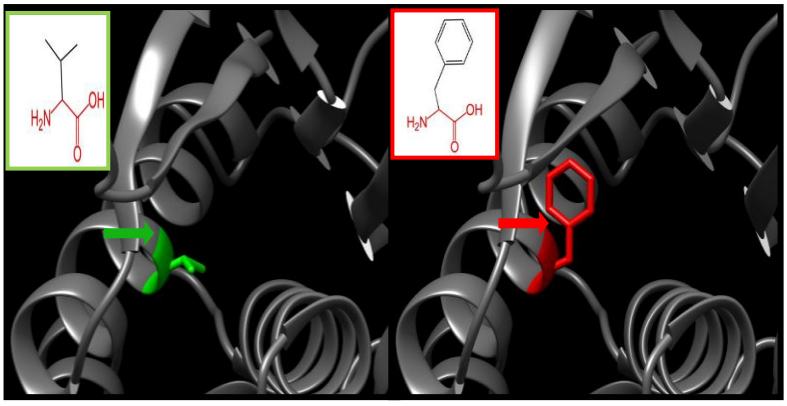

Figure 6: (V50F) the amino acid Valine changes to Phenylalanine at position 50.

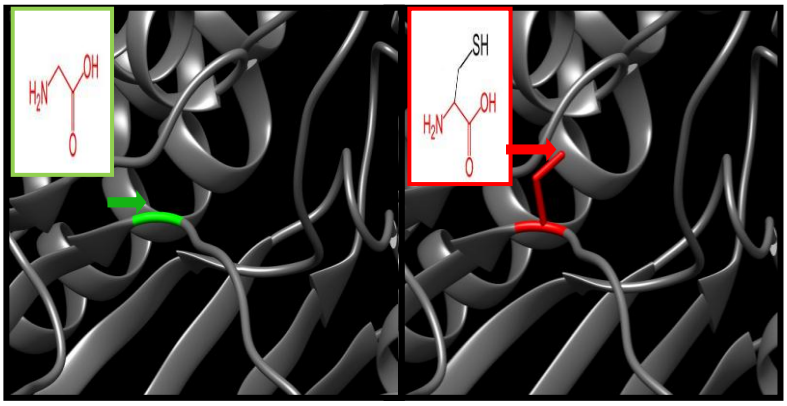

Figure 7: (rs1205294920) (G97C) the amino acid Glycine changes to Cysteine at position 97.

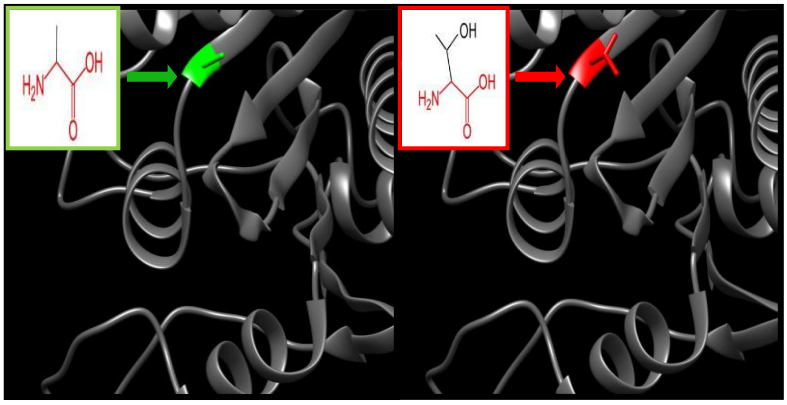

Figure 8: (rs756333430) (A122T) the amino acid Alanine changes to Threonine at position 122.

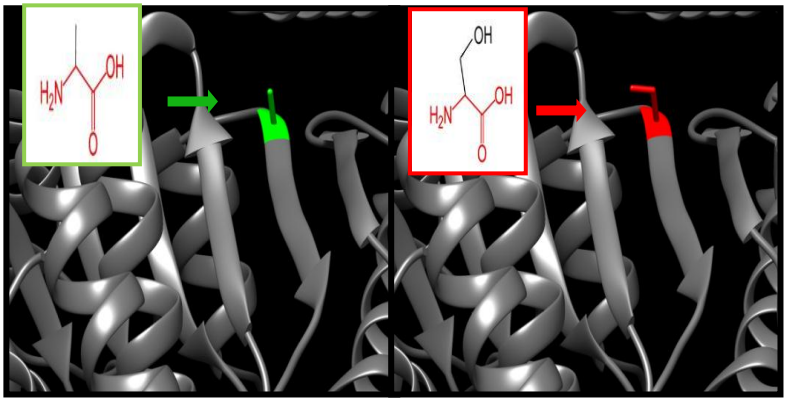

Figure 9: (A122S) the amino acid Alanine changes to Serine at position 122.

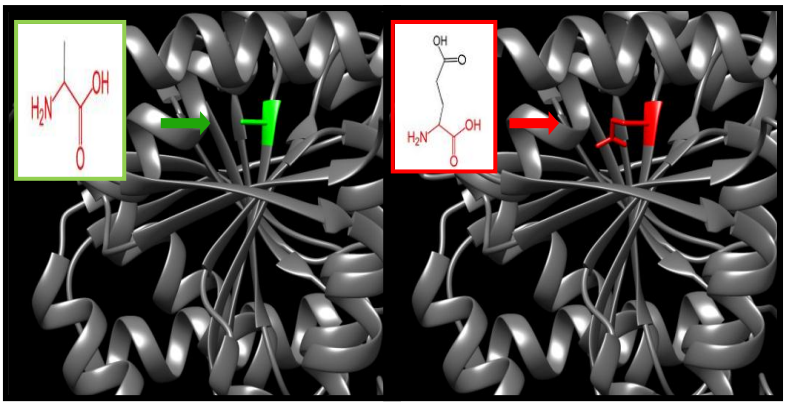

Figure 10: (rs766657715) (A122E) the amino acid Alanine changes to Glutamic Acid at position 122.

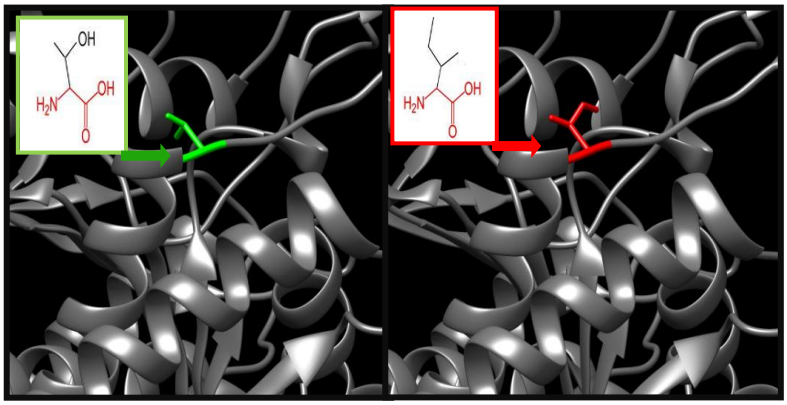

Figure 11: (rs1257538190) (T172I) the amino acid Threonine changes to Isoleucine at position 172.

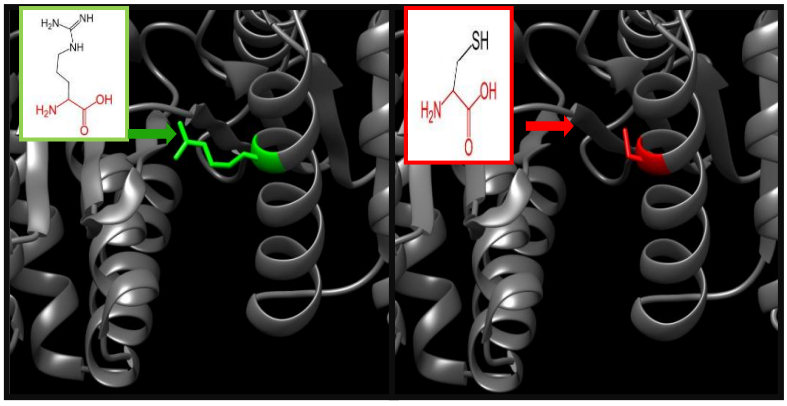

Figure 12 :(rs1404589314) (R178C) the amino acid Arginine changes to Cysteine at position 178.

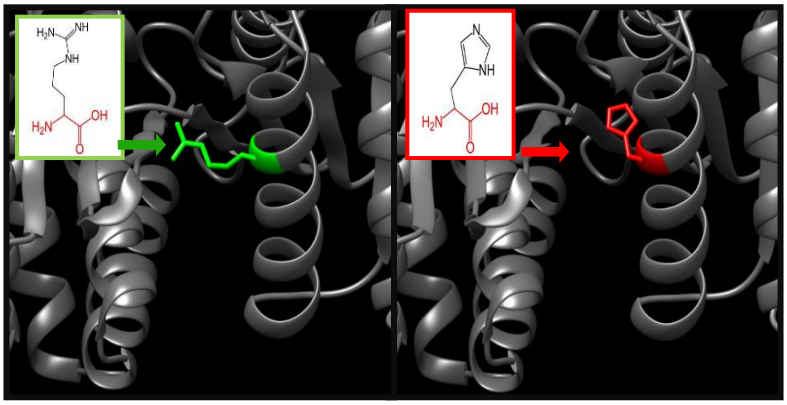

Figure 13: (rs1329563873) (R178H) the amino acid Arginine changes to Histidine at position 178.

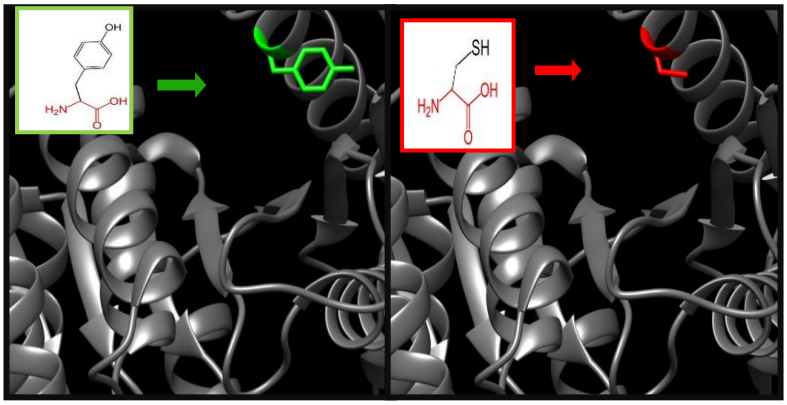

Figure 14: (rs1303775777) (Y186C) the amino acid Tyrosine changes to Cysteine at position 186.

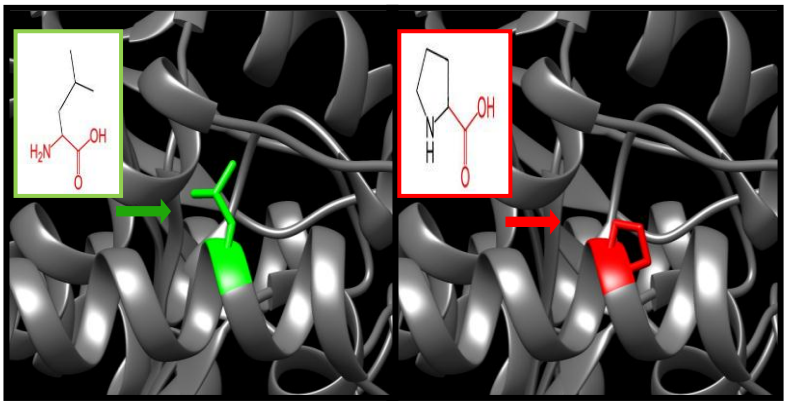

Figure 15: (rs200797531) (V198G) the amino acid Valine changes to Glycine at position 198.

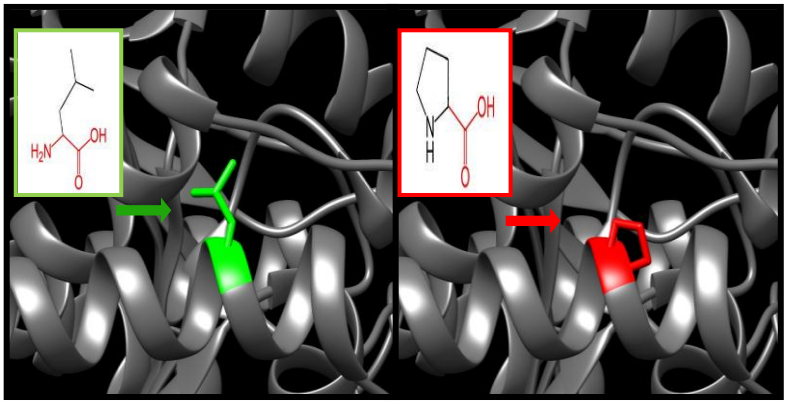

Figure 16: (rs745664361) (L210P) the amino acid Leucine changes to Proline at position 210.

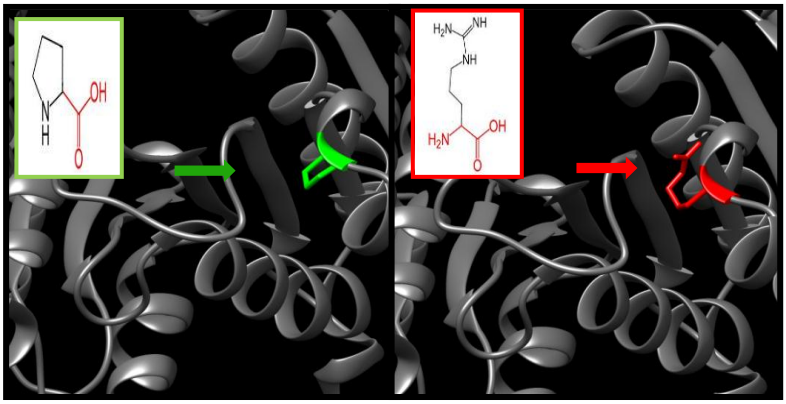

Figure 17: (rs978588480) (P243R) the amino acid Proline changes to Arginine at position 243.

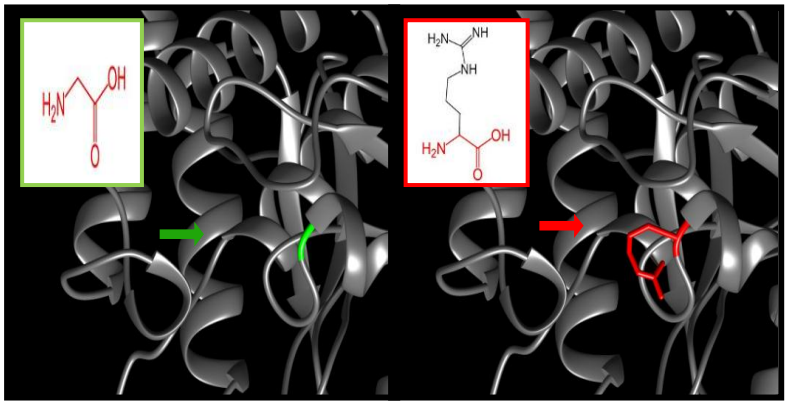

Figure 18: (rs1429951757) (G268R) the amino acid Glycine changes to Arginine at position 268.

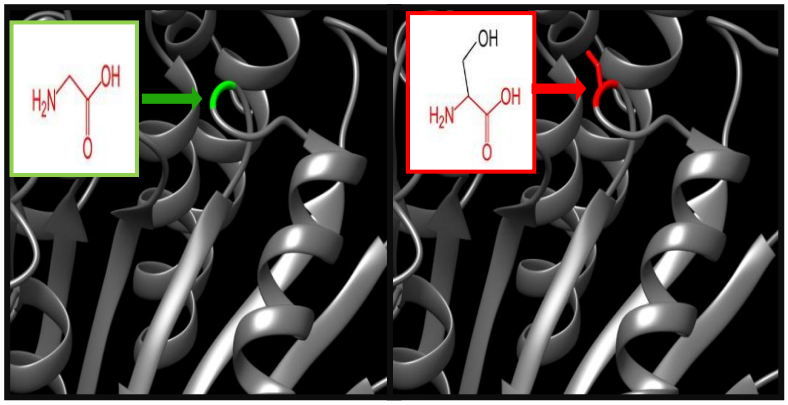

Figure 19: (rs775992590) (G271S) the amino acid Glycine changes to Serine at position 271.

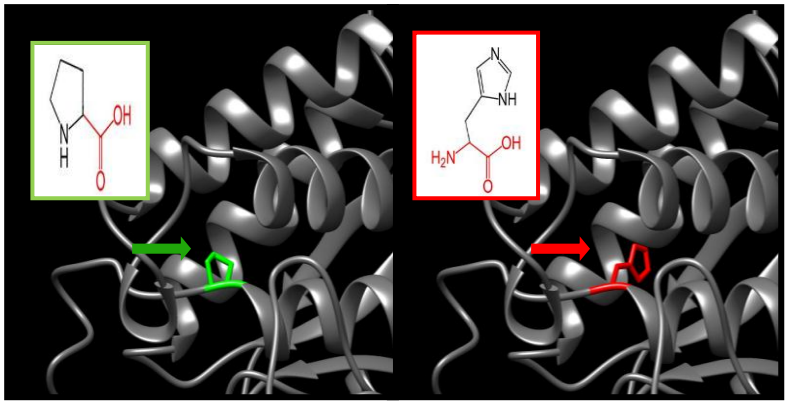

Figure 20: (rs756712426) (P304H) the amino acid Proline changes to Histidine at position 304.

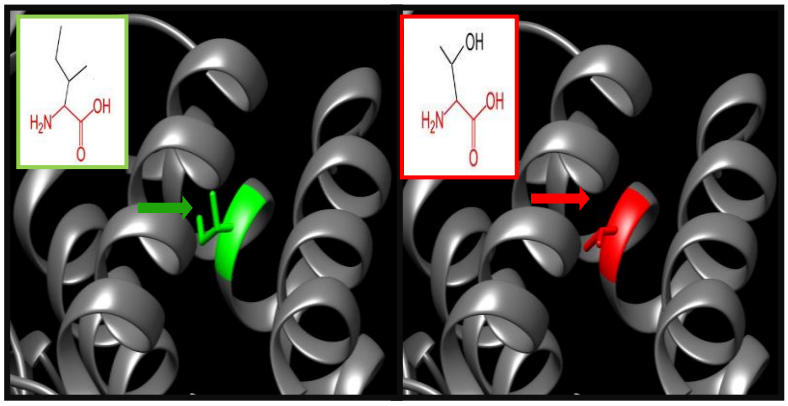

Figure 21: (rs750565047) (I327T) the amino acid Isoleucine changes to Threonine at position 327.

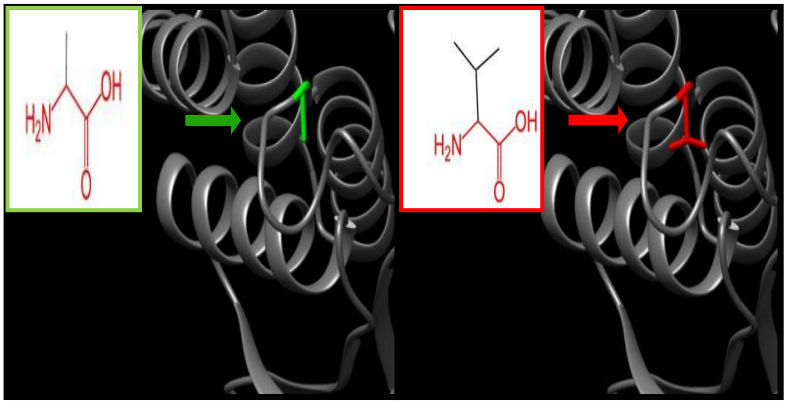

Figure 22: (A302V) the amino acid Alanine changes to Valine at position 302

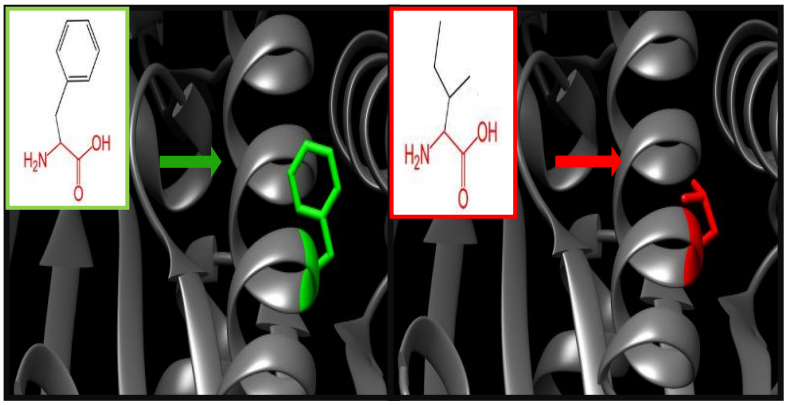

Figure 23: (F184I) the amino acid Phenylalanine changes to Isoleucineat position 184

4. Discussion:

20 novel mutations have been found to affect the stability and function of *IDH3A* gene using bioinformatics tools. The softwares used were based on different aspects and used different parameters to determine the pathogenecity of the SNPs and to give clues about the effect of the mutation on the molecular level. Multiple softwares were used in this study and the results were compared in order to minimize the errors and confirm the results. (Figure 1)

The total number of the nsSNP -571- in Homo sapiens located in the coding region of the *IDH3A* gene was obtained from the dbSNP/NCBI Database; out of this number 178 nsSNPs (missense mutations) were submitted to SIFT server, Polyphen-2 server and provean server respectively to predict the effect of the SNPs on the function of the protein. SIFT server predicted 91 SNPs to be deleterious, polyphen-2 server predicted 90 SNPs to be deleterious (68 probably damaging and 22 possibly damaging) while Provean server predicted 100 deleterious SNPs.

The triple positive results -which are the ones affecting the function of the protein- were found to be 24 SNPs (see table 1); they were submitted to PHD-SNP, SNP&GO and P-MUT for further analysis. 20 deleterious SNPs were predicted by PHD-SNP and SNP&GO while P-MUT predicted 23 deleterious SNPs, so the triple positive result -20 SNPs- (see table 2) was submitted to I-Mutant and MUpro to investigate their effect on the stability.

The 20 SNPs were all found to be decreasing the stability of the protein except for 2 SNPs (F184L and A302V) which were predicted by I-Mutant to increase the stability of the protein (see table 3).

The sequence of *IDH3A* was aligned against 6 members of its homologues using Bioedit software, and all the SNPs were found to be in a conserved region agreeing with the result obtained from Project Hope which revealed that the SNPs are all found in a domain. This suggests that the SNPs will have an effect on the structure and function of the protein. As an example, P304H mutation was found in a conserved region (see figure 3). Project HOPE uncovered that the mutant (Histidine) is bigger than the wild-type (Proline) and the wild-type was buried in the core of the protein so the mutant will probably not fit. In addition to that, there is a difference in the hydrophobicity between the two and the mutation will cause loss of hydrophobic interactions in the core of the protein. This mutation was confirmed pathogenic in our study and that comes with agreement to another study that confirmed the association of P304H mutation with sever encephalopathy in infancy. (28)

GeneMANIA revealed that *IDH3A* interacts with so many genes and functions in the cellular respiration and energy derivation by oxidation of organic compounds in the tricaboxylic acid cycle, and abnormalities in this function was found to play a key role in the pathogenesis of Bipolar Disorder, therefore *IDH3A* could potentially be a novel therapeutic target for bipolar disorder. (29) The genes co-expressed with, share similar protein domain, or participate to achieve similar function were illustrated by GeneMANIA and shown in figure (2) Tables (4 & 5). UCSF Chimera was used to visualize and analysis of molecular structures. (Figures 4-23)

Also aberrant expression of *IDH3A* promotes malignant tumor growth so could be used as a novel target for the diagnosis and treatment of cancers (30, 31).

Our study identified 20 deleterious SNPs that affect the stability and the function of the protein. All these SNPs were retrieved from the NCBI as untested and this study confirmed them damaging. Our study is the first in silico analysis of *IDH3A* gene. It was based on functional analysis while all previous studies (25, 28) were based on exome sequencing. The 20 deleterious SNPs might be considered as a potential novel target in the diagnosis of Retinitis Pigmentosa and associated diseased.

5. **Conclusion**:

In this study the effect of the SNPs of *IDH3A* gene was thoroughly investigated through different bioinformatics prediction softwares. 20 novel mutations were found to have a damaging impact on the structure and function of the protein and may thus be used as diagnostic markers for Retinitis Pigmentosa and could help in the overall understanding of the disease.

Conflict of interest:

The authors declare that they have no competing interest. The authors declare that there is no conflict of interest regarding the publication of this paper.

Acknowledgement:

The authors wish to acknowledge the enthusiastic cooperation of Africa City of Technology-Sudan.

References:

1. Mrejen S, Audo I, Bonnel S, Sahel JA. Retinitis Pigmentosa and Other Dystrophies. Developments in ophthalmology. 2017;58:191-201.
2. Qian TW, Xu X. [Research progress of treatment strategies for retinitis pigmentosa]. [Zhonghua yan ke za zhi] Chinese journal of ophthalmology. 2017;53(2):148-53.
3. He Y, Zhang Y, Su G. Recent advances in treatment of retinitis pigmentosa. Current stem cell research & therapy. 2015;10(3):258-65.
4. Fahim AT, Daiger SP, Weleber RG. Nonsyndromic Retinitis Pigmentosa Overview. In: Adam MP, Ardinger HH, Pagon RA, Wallace SE, Bean LJH, Stephens K, et al., editors. GeneReviews((R)). Seattle (WA): University of Washington, Seattle

University of Washington, Seattle. GeneReviews is a registered trademark of the University of Washington, Seattle. All rights reserved.; 1993.
5. Dias MF, Joo K, Kemp JA, Fialho SL, da Silva Cunha A, Jr., Woo SJ, et al. Molecular genetics and emerging therapies for retinitis pigmentosa: Basic research and clinical perspectives. Progress in retinal and eye research. 2018;63:107-31.
6. Petit L, Punzo C. mTORC1 sustains vision in retinitis pigmentosa. Oncotarget. 2015;6(19):16786-7.
7. Wang M, Gan D, Huang X, Xu G. Novel compound heterozygous mutations in CNGA1in a Chinese family affected with autosomal recessive retinitis pigmentosa by targeted sequencing. BMC ophthalmology. 2016;16:101.
8. Chang S, Vaccarella L, Olatunji S, Cebulla C, Christoforidis J. Diagnostic challenges in retinitis pigmentosa: genotypic multiplicity and phenotypic variability. Current genomics. 2011;12(4):267-75.
9. Enani L, Kozak I, Abdelkader E. A Case of Unilateral Retinitis Pigmentosa Associated with Full Thickness Macular Hole. Middle East African journal of ophthalmology. 2017;24(2):113-5.
10. Marchena M, Villarejo-Zori B, Zaldivar-Diez J, Palomo V, Gil C, Hernandez-Sanchez C, et al. Small molecules targeting glycogen synthase kinase 3 as potential drug candidates for the treatment of retinitis pigmentosa. Journal of enzyme inhibition and medicinal chemistry. 2017;32(1):522-6.
11. Wang DY, Chan WM, Tam PO, Chiang SW, Lam DS, Chong KK, et al. Genetic markers for retinitis pigmentosa. Hong Kong medical journal = Xianggang yi xue za zhi. 2005;11(4):281-8.
12. Al-Khersan H, Shah KP, Jung SC, Rodriguez A, Madduri RK, Grassi MA. A novel MERTK mutation causing retinitis pigmentosa. Graefe's archive for clinical and experimental ophthalmology = Albrecht von Graefes Archiv fur klinische und experimentelle Ophthalmologie. 2017;255(8):1613-9.
13. Zhang Y, Guo X, Wang M, Wang L, Tian Q, Zheng D, et al. Reduced Field-of-View Diffusion Tensor Imaging of the Optic Nerve in Retinitis Pigmentosa at 3T. AJNR American journal of neuroradiology. 2016;37(8):1510-5.
14. O'Neal TB, Luther EE. Retinitis Pigmentosa. StatPearls. Treasure Island (FL): StatPearls Publishing

StatPearls Publishing LLC.; 2018.
15. Verbakel SK, van Huet RAC, Boon CJF, den Hollander AI, Collin RWJ, Klaver CCW, et al. Non-syndromic retinitis pigmentosa. Progress in retinal and eye research. 2018;66:157-86.
16. Xu M, Yamada T, Sun Z, Eblimit A, Lopez I, Wang F, et al. Mutations in POMGNT1 cause non-syndromic retinitis pigmentosa. Human molecular genetics. 2016;25(8):1479-88.
17. Nagase Y, Kurata K, Hosono K, Suto K, Hikoya A, Nakanishi H, et al. Visual Outcomes in Japanese Patients with Retinitis Pigmentosa and Usher Syndrome Caused by USH2A Mutations. Seminars in ophthalmology. 2018;33(4):560-5.

18. Pierrottet CO, Zuntini M, Digiuni M, Bazzanella I, Ferri P, Paderni R, et al. Syndromic and non-syndromic forms of retinitis pigmentosa: a comprehensive Italian clinical and molecular study reveals new mutations. Genetics and molecular research : GMR. 2014;13(4):8815-33.
19. Ali MU, Rahman MSU, Cao J, Yuan PX. Genetic characterization and disease mechanism of retinitis pigmentosa; current scenario. 3 Biotech. 2017;7(4):251.
20. Hartong DT, Berson EL, Dryja TP. Retinitis pigmentosa. Lancet (London, England). 2006;368(9549):1795-809.
21. Sullivan LS, Bowne SJ, Birch DG, Hughbanks-Wheaton D, Heckenlively JR, Lewis RA, et al. Prevalence of disease-causing mutations in families with autosomal dominant retinitis pigmentosa: a screen of known genes in 200 families. Investigative ophthalmology & visual science. 2006;47(7):3052-64.
22. Daiger SP, Bowne SJ, Sullivan LS. Perspective on genes and mutations causing retinitis pigmentosa. Archives of ophthalmology (Chicago, Ill : 1960). 2007;125(2):151-8.
23. Daiger SP, Sullivan LS, Gire AI, Birch DG, Heckenlively JR, Bowne SJ. Mutations in known genes account for 58% of autosomal dominant retinitis pigmentosa (adRP). Advances in experimental medicine and biology. 2008;613:203-9.
24. Pelletier V, Jambou M, Delphin N, Zinovieva E, Stum M, Gigarel N, et al. Comprehensive survey of mutations in RP2 and RPGR in patients affected with distinct retinal dystrophies: genotype-phenotype correlations and impact on genetic counseling. Human mutation. 2007;28(1):81-91.
25. Pierrache LHM, Kimchi A, Ratnapriya R, Roberts L, Astuti GDN, Obolensky A, et al. Whole-Exome Sequencing Identifies Biallelic IDH3A Variants as a Cause of Retinitis Pigmentosa Accompanied by Pseudocoloboma. Ophthalmology. 2017;124(7):992-1003.
26. Huh TL, Kim YO, Oh IU, Song BJ, Inazawa J. Assignment of the human mitochondrial NAD+ -specific isocitrate dehydrogenase alpha subunit (IDH3A) gene to 15q25.1-->q25.2by in situ hybridization. Genomics. 1996;32(2):295-6.
27. Soundar S, Park JH, Huh TL, Colman RF. Evaluation by mutagenesis of the importance of 3 arginines in alpha, beta, and gamma subunits of human NAD-dependent isocitrate dehydrogenase. The Journal of biological chemistry. 2003;278(52):52146-53.
28. Fattal-Valevski A, Eliyahu H, Fraenkel ND, Elmaliach G, Hausman-Kedem M, Shaag A, et al. Homozygous mutation, p.Pro304His, in IDH3A, encoding isocitrate dehydrogenase subunit is associated with severe encephalopathy in infancy. Neurogenetics. 2017;18(1):57-61.
29. Yoshimi N, Futamura T, Bergen SE, Iwayama Y, Ishima T, Sellgren C, et al. Cerebrospinal fluid metabolomics identifies a key role of isocitrate dehydrogenase in bipolar disorder: evidence in support of mitochondrial dysfunction hypothesis. Molecular psychiatry. 2016;21(11):1504-10.
30. O'Brien TD, Jia P, Caporaso NE, Landi MT, Zhao Z. Weak sharing of genetic association signals in three lung cancer subtypes: evidence at the SNP, gene, regulation, and pathway levels. Genome medicine. 2018;10(1):16.
31. Zeng L, Morinibu A, Kobayashi M, Zhu Y, Wang X, Goto Y, et al. Aberrant IDH3alpha expression promotes malignant tumor growth by inducing HIF-1-mediated metabolic reprogramming and angiogenesis. Oncogene. 2015;34(36):4758-66.
32. Strong S, Liew G, Michaelides M. Retinitis pigmentosa-associated cystoid macular oedema: pathogenesis and avenues of intervention. The British journal of ophthalmology. 2017;101(1):31-7.
33. Liu YP, Bosch DG, Siemiatkowska AM, Rendtorff ND, Boonstra FN, Moller C, et al. Putative digenic inheritance of heterozygous RP1L1 and C2orf71 null mutations in syndromic retinal dystrophy. Ophthalmic genetics. 2017;38(2):127-32.
34. Haer-Wigman L, Newman H, Leibu R, Bax NM, Baris HN, Rizel L, et al. Non-syndromic retinitis pigmentosa due to mutations in the mucopolysaccharidosis type IIIC gene, heparan-alpha-glucosaminide N-acetyltransferase (HGSNAT). Human molecular genetics. 2015;24(13):3742-51.

35. Nguyen TT, Hull S, Roepman R, van den Born LI, Oud MM, de Vrieze E, et al. Missense mutations in the WD40 domain of AHI1 cause non-syndromic retinitis pigmentosa. Journal of medical genetics. 2017;54(9):624-32.
36. Dutta Majumder P, Menia N, Roy R, Sen P, A EG, S KG, et al. Uveitis in Patients with Retinitis Pigmentosa: 30 Years' Consecutive Data. Ocular immunology and inflammation. 2018;26(8):1283-8.
37. Sacchetti M, Mantelli F, Merlo D, Lambiase A. Systematic Review of Randomized Clinical Trials on Safety and Efficacy of Pharmacological and Nonpharmacological Treatments for Retinitis Pigmentosa. Journal of ophthalmology. 2015;2015:737053.
38. Tenenbaum JD. Translational Bioinformatics: Past, Present, and Future. Genomics, proteomics & bioinformatics. 2016;14(1):31-41.
39. Database resources of the National Center for Biotechnology Information. Nucleic acids research. 2018;46(D1):D8-d13.
40. Sherry ST, Ward MH, Kholodov M, Baker J, Phan L, Smigielski EM, et al. dbSNP: the NCBI database of genetic variation. Nucleic acids research. 2001;29(1):308-11.
41. UniProt: the universal protein knowledgebase. Nucleic acids research. 2017;45(D1):D158-d69.
42. Schneider G, Hu J, Sim N-L, Kumar P, Henikoff S, Ng PC. SIFT web server: predicting effects of amino acid substitutions on proteins. Nucleic acids research. 2012;40(W1):W452-W7.
43. Ng PC, Henikoff S. SIFT: Predicting amino acid changes that affect protein function. Nucleic acids research. 2003;31(13):3812-4.
44. Adzhubei IA, Schmidt S, Peshkin L, Ramensky VE, Gerasimova A, Bork P, et al. A method and server for predicting damaging missense mutations. Nature methods. 2010;7(4):248-9.
45. Ramensky V, Bork P, Sunyaev S. Human non-synonymous SNPs: server and survey. Nucleic acids research. 2002;30(17):3894-900.
46. Choi Y, Sims GE, Murphy S, Miller JR, Chan AP. Predicting the functional effect of amino acid substitutions and indels. PloS one. 2012;7(10):e46688.
47. Choi Y, Chan AP. PROVEAN web server: a tool to predict the functional effect of amino acid substitutions and indels. Bioinformatics. 2015;31(16):2745-7.
48. Capriotti E, Calabrese R, Fariselli P, Martelli PL, Altman RB, Casadio R. WS-SNPs&GO: a web server for predicting the deleterious effect of human protein variants using functional annotation. BMC genomics. 2013;14 Suppl 3:S6.
49. Capriotti E, Martelli PL, Fariselli P, Casadio R. Blind prediction of deleterious amino acid variations with SNPs&GO. Human mutation. 2017;38(9):1064-71.
50. Ferrer-Costa C, Gelpi JL, Zamakola L, Parraga I, de la Cruz X, Orozco M. PMUT: a web-based tool for the annotation of pathological mutations on proteins. Bioinformatics. 2005;21(14):3176-8.
51. Capriotti E, Fariselli P, Casadio R. I-Mutant2.0: predicting stability changes upon mutation from the protein sequence or structure. Nucleic acids research. 2005;33(Web Server issue):W306-10.
52. Pettersen EF, Goddard TD, Huang CC, Couch GS, Greenblatt DM, Meng EC, et al. UCSF Chimera--a visualization system for exploratory research and analysis. Journal of computational chemistry. 2004;25(13):1605-12.
53. Franz M, Rodriguez H, Lopes C, Zuberi K, Montojo J, Bader GD, et al. GeneMANIA update 2018. Nucleic acids research. 2018;46(W1):W60-w4.
54. Warde-Farley D, Donaldson SL, Comes O, Zuberi K, Badrawi R, Chao P, et al. The GeneMANIA prediction server: biological network integration for gene prioritization and predicting gene function. Nucleic acids research. 2010;38(Web Server issue):W214-20.
55. Montojo J, Zuberi K, Rodriguez H, Kazi F, Wright G, Donaldson SL, et al. GeneMANIA Cytoscape plugin: fast gene function predictions on the desktop. Bioinformatics. 2010;26(22):2927-8.

56. Venselaar H, Te Beek TA, Kuipers RK, Hekkelman ML, Vriend G. Protein structure analysis of mutations causing inheritable diseases. An e-Science approach with life scientist friendly interfaces. BMC bioinformatics. 2010;11:548.